

Analysis of diffuse damage to localized cracking in saturated porous materials with a micro-mechanics based friction-damage approach

Jianfu Shao^{1,3}, Lunyang Zhao², Qizhi Zhu³

¹University of Lille, CNRS, Centrale Lille, LaMcube, UMR9013, France

²School of Civil Engineering and Transportation, South China University of Technology, China

³College of Civil and Transportation Engineering, Hohai University, China

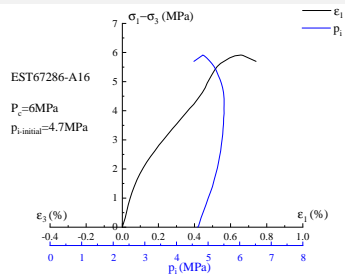
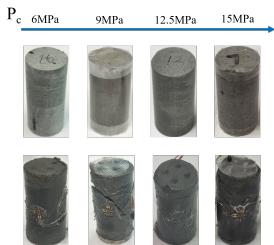
Table of Contents

- 1 Motivation and objective
- 2 Micromechanics-based friction-damage model with pore pressure effect
- 3 Friction-damage modelling based on localized crack
- 4 Analysis of cracking localization
- 5 Numerical simulation of porous quasi-brittle materials
- 6 Conclusions and perspectives

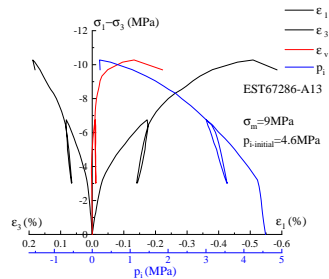
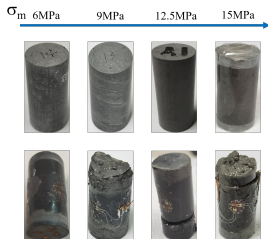
Table of Contents

- 1 Motivation and objective
- 2 Micromechanics-based friction-damage model with pore pressure effect
- 3 Friction-damage modelling based on localized crack
- 4 Analysis of cracking localization
- 5 Numerical simulation of porous quasi-brittle materials
- 6 Conclusions and perspectives

Crack initiation and propagation in rocks



Cracking pattern of COx claystone in triaxial compression tests (Zhang et al. 2023)

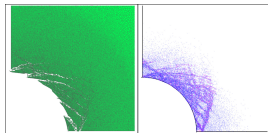


Cracking pattern of COx claystone in triaxial extension tests (Zhang et al. 2023)

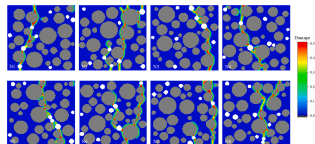
Principal methods for cracking modeling

Nucleation and propagation of cracks: key mechanism of failure and instability of geomaterials and related structures

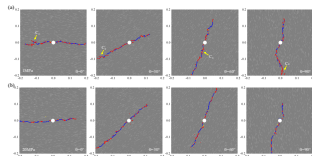
- cracks seen as localization bands (weak discontinuity): bifurcation theory, high order gradient models, non-local damage models;
- discrete methods: DEM, Peridynamics theory, RBS (rigid block spring) method, etc.
- Boundary element method;
- Finite element methods: XFEM, EFEM, Phase-field



(Yao, Shao et al. 2017)



(Jin et al. 2021)



(Zhang, Shao et al. 2022)

Cracking modeling with finite element framework -1

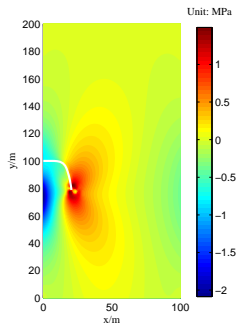
Extended finite element method (XFEM):

- Global enrichment of displacement discontinuity (Moes et al. 1999):

$$u^h(x) = \sum_{I \in N} N_I(x) u_I + \sum_{I \in N^{cr}} N_I(x) (H(\varphi(x)) - H(\varphi(x_I))) a_I \\ + \sum_{I \in N^{tip}} N_I(x) \sum_{k=1}^4 (F^k(x) - F^k(x_I)) b_I^k$$

- Enriched tip element function (Belytschko and Black, 1999):

$$\{F\} = \left[\sqrt{r} \cos \frac{\theta_1}{2} \sqrt{g_1(\theta)} \sqrt{r} \cos \frac{\theta_2}{2} \sqrt{g_2(\theta)}, \sqrt{r} \sin \frac{\theta_1}{2} \sqrt{g_1(\theta)}, \sqrt{r} \sin \frac{\theta_2}{2} \sqrt{g_2(\theta)} \right]$$

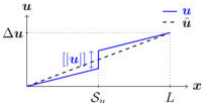
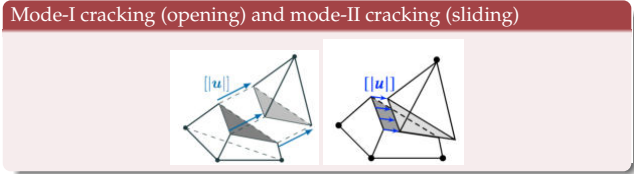


Nucleation of new cracks; crack growth extent, orientation for 3D multiple cracks; change of DOF

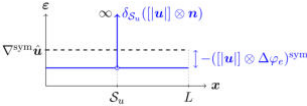
Cracking modeling with finite element framework -2

EFEM - Enriched finite element method (Oliver 1996; Sun et al. 2021a, 2021b): Elementary enrichment of displacement discontinuity

Discontinuity : jump in the displacement field (cracking)



$$\mathbf{u} = \underbrace{\hat{\mathbf{u}}}_{\text{regular part}} + \underbrace{(\mathcal{H}_{S_u} - \phi_e)[\mathbf{u}]}_{\text{enhanced part}}$$



$$\boldsymbol{\varepsilon} = \underbrace{\nabla^S(\hat{\mathbf{u}})}_{\text{regular part}} + \underbrace{\mathbf{G}_s[\mathbf{u}]}_{\text{enhanced part}}$$

No transition from diffuse damage to localized cracking; difficult combination of tensile and shear cracks

Variational non-local damage approach - Phase-field models

Variational approach of fracture mechanics (Francfort and Marigo 1998; Bourdin et al. 2000) Approximation of sharp crack surface area by smeared crack field $d(\mathbf{x}) \in [0, 1]$:

$$A_{\Gamma} = \int_{\Gamma^k} dA \implies A_{\Gamma_l}(d) = \int_{\Omega} \gamma(d, \nabla d) d\Omega$$

Total energy functional:

$$E(\boldsymbol{\varepsilon}(\mathbf{u}), \boldsymbol{\varepsilon}^p, \mathbf{V}^p, d) = \int_{\Omega} \psi(\boldsymbol{\varepsilon}, \boldsymbol{\varepsilon}^p, \mathbf{V}^p, d) dV + \mathcal{D}_c + \int_{\Omega} \beta(d) \int_0^t \varphi(\dot{\boldsymbol{\varepsilon}}^p, \dot{\mathbf{V}}^p) d\tau dV$$

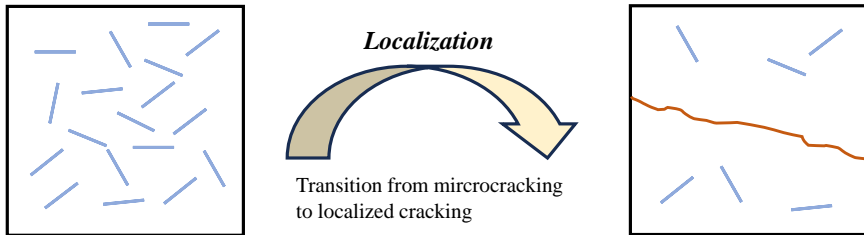
Dissipated energy during crack growth \mathcal{D}_c :

$$\mathcal{D}_c = \int_{\Omega} g_c \gamma(d, \nabla d) dV$$

Minimization of the total energy functional and crack evolution law:

$$\frac{\partial}{\partial d} \psi(\boldsymbol{\varepsilon}, \boldsymbol{\varepsilon}^p, \mathbf{V}^p, d) + \beta'(d) \mathcal{D}_p + \frac{g_c}{l_d} d - g_c l_d \operatorname{div}(\nabla d) = 0$$

Objective: Micro-mechanics based damage-friction model



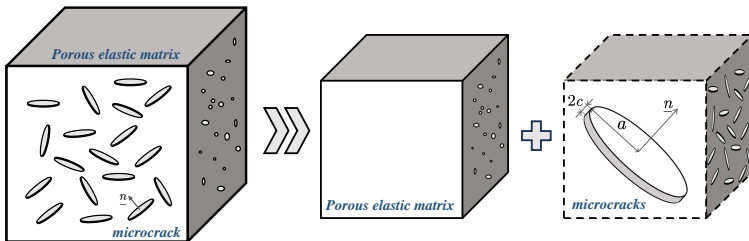
Transition from diffuse damage to localized cracking in saturated porous media by considering coupling between microcrack growth and frictional sliding.

- Establishing the poroelastic relations of cracked media
- Thermodynamics framework for microcrack propagation and frictional sliding, with the fluid pressure effect
- Modeling of localized cracks at elementary level with homogenization procedure

Table of Contents

- 1 Motivation and objective
- 2 Micromechanics-based friction-damage model with pore pressure effect**
- 3 Friction-damage modelling based on localized crack
- 4 Analysis of cracking localization
- 5 Numerical simulation of porous quasi-brittle materials
- 6 Conclusions and perspectives

RVE of porous materials with diffuse micro-cracks



$$E = E^m + E^c$$

Homogenized poroelastic law:

$$(\Sigma + B P_w) = C^{hom} : E = C^m : (E - E^c) , B = \delta - C^{hom} : S^s : \delta$$

Macroscopic elastic stiffness tensor:

$$C^{hom} = C^m + \varphi^c (C^c - C^m) : A^c = 3k^{hom} J + 2\mu^{hom} K ; S^{hom} = (C^{hom})^{-1} = S^m + S^f$$

with the MT scheme for isotropic matrix with open microcracks:

$$C^{hom} = \frac{1}{1 + \eta_1 d} 3k^m J + \frac{1}{1 + \eta_2 d} 2\mu^m K , \eta_1 = \frac{16}{9} \frac{1 - (\nu^m)^2}{1 - 2\nu^m} , \eta_2 = \frac{32}{45} \frac{(1 - \nu^m)(5 - \nu^m)}{1 - 2\nu^m}$$

Damage-friction coupling in closed microcracks

Free energy function (continuity between open and closed microcrack):

$$\Psi^u = \frac{1}{2} (\mathbf{E} - \mathbf{E}^c) : \mathbb{C}^u : (\mathbf{E} - \mathbf{E}^c) + \frac{1}{2} \mathbf{E}^c : \mathbb{C}^f : \mathbf{E}^c - M \left(\frac{m}{\rho_f^0} - \phi^p \right) \mathbf{B} : (\mathbf{E} - \mathbf{E}^c) + \frac{M}{2} \left(\frac{m}{\rho_f^0} - \phi^p \right)^2$$

Equivalently:

$$\Psi = \frac{1}{2} (\mathbf{E} - \mathbf{E}^c) : \mathbb{C}^m : (\mathbf{E} - \mathbf{E}^c) + \frac{1}{2} \mathbf{E}^c : \mathbb{C}^f : \mathbf{E}^c - \frac{1}{2} N P_w^2 - P_w (\mathbf{E} - \mathbf{E}^c) : \mathbf{B} - P_w \mathbf{E}^c : \boldsymbol{\delta}$$

$$\mathbb{C}^u = \mathbb{C}^m + M(\mathbf{B} \otimes \mathbf{B}), \quad \frac{1}{N} = (\mathbf{B} - \phi \mathbf{I}) : \mathbb{S}^m : \mathbf{I}, \quad \frac{1}{M} = \frac{1}{N} + \frac{\phi}{k_f}, \quad \mathbb{C}^f = \frac{1}{\eta_1 d} 3k^m \mathbb{J} + \frac{1}{\eta_2 d} 2\mu^m \mathbb{K}$$

Damage-friction coupling in closed microcracks

Free energy function (continuity between open and closed microcrack):

$$\Psi^u = \frac{1}{2} (\mathbf{E} - \mathbf{E}^c) : \mathbb{C}^u : (\mathbf{E} - \mathbf{E}^c) + \frac{1}{2} \mathbf{E}^c : \mathbb{C}^f : \mathbf{E}^c - M \left(\frac{m}{\rho_f^0} - \phi^p \right) \mathbf{B} : (\mathbf{E} - \mathbf{E}^c) + \frac{M}{2} \left(\frac{m}{\rho_f^0} - \phi^p \right)^2$$

Equivalently:

$$\Psi = \frac{1}{2} (\mathbf{E} - \mathbf{E}^c) : \mathbb{C}^m : (\mathbf{E} - \mathbf{E}^c) + \frac{1}{2} \mathbf{E}^c : \mathbb{C}^f : \mathbf{E}^c - \frac{1}{2} NP_w^2 - P_w (\mathbf{E} - \mathbf{E}^c) : \mathbf{B} - P_w \mathbf{E}^c : \boldsymbol{\delta}$$

$$\mathbb{C}^u = \mathbb{C}^m + M(\mathbf{B} \otimes \mathbf{B}), \quad \frac{1}{N} = (\mathbf{B} - \phi \mathbf{I}) : \mathbb{S}^m : \mathbf{I}, \quad \frac{1}{M} = \frac{1}{N} + \frac{\phi}{k_f}, \quad \mathbb{C}^f = \frac{1}{\eta_1 d} 3k^m \mathbb{J} + \frac{1}{\eta_2 d} 2\mu^m \mathbb{K}$$

- State equations

$$\boldsymbol{\Sigma} = \mathbb{C}^m : (\mathbf{E} - \mathbf{E}^c) - \mathbf{B} P_w$$

$$(\phi - \phi_0 - \phi^p) = \frac{\partial (\Psi - \Psi^c)}{\partial P_w} = NP_w + (\mathbf{E} - \mathbf{E}^c) : \mathbf{B}$$

$$(P_w - P_{w,0}) = -\frac{\partial \Psi^u}{\partial \phi^p} = M \left[\left(\frac{m_f}{\rho_f^0} - \phi^p \right) - (\mathbf{E} - \mathbf{E}^c) : \mathbf{B} \right]$$

- Conjugate forces related to damage and friction

$$\mathcal{Y}^d = -\frac{\partial \Psi}{\partial d} = -\frac{1}{2} \mathbf{E}^c : \frac{\partial \mathbb{C}^f}{\partial d} : \mathbf{E}^c, \quad \boldsymbol{\Sigma}^c = -\frac{\partial \Psi}{\partial \mathbf{E}^c} = (\boldsymbol{\Sigma} + P_w \boldsymbol{\delta}) - \mathbb{C}^f : \mathbf{E}^c$$

Evolution of pore fluid pressure:

- An effective form of pore-plasticity:

$$\phi^p = \beta \text{tr}(\mathbf{E}^c) = \beta \mathbf{E}^c : \boldsymbol{\delta}$$

The coefficient β generally determined from experimental data.

- Incremental of interstitial fluid pressure (zero at drained tests)

$$dP_w = M [- (d\mathbf{E} - d\mathbf{E}^c) : \mathbf{B} - \beta d\mathbf{E}^c : \boldsymbol{\delta}]$$

- Evolution of porosity

$$(\phi - \phi_0) = NP_w + (\mathbf{E} - \mathbf{E}^c) : \mathbf{B} + \beta \mathbf{E}^c : \boldsymbol{\delta}$$

Evolution of pore fluid pressure:

- An effective form of pore-plasticity:

$$\phi^p = \beta \text{tr}(\mathbf{E}^c) = \beta \mathbf{E}^c : \boldsymbol{\delta}$$

The coefficient β generally determined from experimental data.

- Incremental of interstitial fluid pressure (zero at drained tests)

$$dP_w = M [- (d\mathbf{E} - d\mathbf{E}^c) : \mathbf{B} - \beta d\mathbf{E}^c : \boldsymbol{\delta}]$$

- Evolution of porosity

$$(\phi - \phi_0) = NP_w + (\mathbf{E} - \mathbf{E}^c) : \mathbf{B} + \beta \mathbf{E}^c : \boldsymbol{\delta}$$

Frictional sliding and damage growth:

- Friction criterion with local stress tensor

$$\mathcal{F}(\boldsymbol{\Sigma}^c) = \|\mathbf{S}^c\| + \eta_f \Sigma_m^c \leq 0 \quad \text{with} \quad \boldsymbol{\Sigma}^c = (\boldsymbol{\Sigma} + P_w \boldsymbol{\delta}) - \mathbb{C}^f : \mathbf{E}^c$$

- Damage criterion based on the concept of energy release rate

$$\mathcal{G}(\mathcal{Y}^d, d) = \mathcal{Y}^d - \mathcal{R}(d) \leq 0 \quad \text{with} \quad \mathcal{R}(d) = \frac{2\xi}{1 + \xi^2} \mathcal{R}(d_c), \quad \xi = \frac{d}{d_c}$$

$\mathcal{R}(d_c)$ equivalent critical toughness for onset of localized crack!

Table of Contents

- 1 Motivation and objective
- 2 Micromechanics-based friction-damage model with pore pressure effect
- 3 Friction-damage modelling based on localized crack**
- 4 Analysis of cracking localization
- 5 Numerical simulation of porous quasi-brittle materials
- 6 Conclusions and perspectives

Free energy with localized crack

$$\begin{aligned}\tilde{\Psi} = & \frac{1}{2} \left(\mathbf{E} - \mathbf{E}^{c,l} - \tilde{\mathbf{E}}^c \right) : \mathbb{C}^m : \left(\mathbf{E} - \mathbf{E}^{c,l} - \tilde{\mathbf{E}}^c \right) + \frac{1}{2} \mathbf{E}^{c,l} : \mathbb{C}^{f,l} : \mathbf{E}^{c,l} + \frac{1}{2} \tilde{\mathbf{E}}^c : \mathbb{C}^n : \tilde{\mathbf{E}}^c \\ & - \frac{1}{2} NP_w^2 - P_w \left(\mathbf{E} - \mathbf{E}^{c,l} - \tilde{\mathbf{E}}^c \right) : \mathbf{B} - P_w \delta : \left(\mathbf{E}^{c,l} + \tilde{\mathbf{E}}^c \right)\end{aligned}$$

- State equations with localized crack:

$$\boldsymbol{\Sigma} = \frac{\partial \tilde{\Psi}}{\partial \mathbf{E}} = \mathbb{C}^m : \left(\mathbf{E} - \mathbf{E}^{c,l} - \tilde{\mathbf{E}}^c \right) - P_w \mathbf{B}$$

$$(\phi - \phi_0) = NP_w + \left(\mathbf{E} - \mathbf{E}^{c,l} - \tilde{\mathbf{E}}^c \right) : \mathbf{B} + \phi_0 \left(\mathbf{E}^{c,l} + \tilde{\mathbf{E}}^c \right) : \boldsymbol{\delta}$$

$$(P_w - P_{w,0}) = M \left[\left(\frac{m_f}{\rho_f^0} - \phi_0 \left(\mathbf{E}^{c,l} + \tilde{\mathbf{E}}^c \right) : \boldsymbol{\delta} \right) - \left(\mathbf{E} - \mathbf{E}^{c,l} - \tilde{\mathbf{E}}^c \right) : \mathbf{B} \right]$$

- Thermodynamic forces for localized crack:

$$\tilde{\boldsymbol{\Sigma}}^c = \frac{\partial \tilde{\Psi}}{\partial \tilde{\mathbf{E}}^c} = (\boldsymbol{\Sigma} + P_w \boldsymbol{\delta}) - \mathbb{C}^n : \tilde{\mathbf{E}}^c$$

$$\tilde{\mathcal{Y}}^d = -\frac{\partial \tilde{\Psi}}{\partial d} = -\frac{1}{2} \tilde{\mathbf{E}}^c : \frac{\partial \mathbb{C}^n}{\partial d} : \tilde{\mathbf{E}}^c$$

Frictional sliding and growth of localized crack

- Friction criterion of localized crack

$$\tilde{\mathcal{F}}\left(\tilde{\Sigma}^c\right) = \|\tilde{\tau}^c\| + \tilde{\eta}_f \tilde{\Sigma}_n^c \leq 0$$

where

$$\tilde{\tau}^c = \tilde{\Sigma}^c \cdot \underline{n} \cdot \mathbf{T} = \underline{\tau} - \underline{n} \cdot \mathbf{T} \cdot \mathbb{C}^n : \tilde{\mathbf{E}}^c ; \quad \tilde{\Sigma}_n^c = \underline{n} \cdot \tilde{\Sigma}^c \cdot \underline{n} = \Sigma_n - \mathbf{N} : \mathbb{C}^n : \tilde{\mathbf{E}}^c + P_w$$

If no rotation of principal axes in conventional triaxial compression, flow direction simplified as

$$\underline{t} = \frac{\underline{\tau}}{\|\tau\|} = \text{sign}(\Sigma_1 - \Sigma_3) \frac{\underline{e}_1 - (\underline{e}_1 \cdot \underline{n}) \underline{n}}{\sqrt{1 - \underline{e}_1 \cdot \underline{n}}} \quad \text{so that} \quad \|\tilde{\tau}^c\| = \tilde{\tau}^c \cdot \underline{t}$$

- Non-associated frictional flow - friction-induced dilatancy:

$$\tilde{\mathcal{F}}_p\left(\tilde{\Sigma}^c\right) = \|\tilde{\tau}^c\| + \beta_d \tilde{\eta}_f \tilde{\Sigma}_n^c \leq 0 \quad \text{with} \quad \mathbf{V} = \frac{\partial \tilde{\mathcal{F}}_p}{\partial \tilde{\Sigma}^c} = \underline{t} \otimes \underline{n} + \beta_d \tilde{\eta}_f \mathbf{N}$$

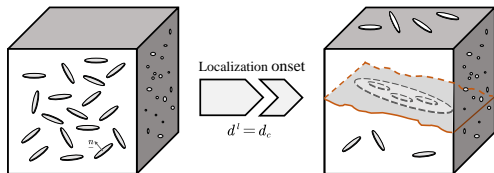
- Evolution of localized crack

$$\tilde{\mathcal{G}}\left(\tilde{\mathcal{Y}}^d, d\right) = \tilde{\mathcal{Y}}^d - \tilde{\mathcal{R}}(d) = 0 \quad \text{with} \quad \tilde{\mathcal{R}}(d) = \frac{2\xi}{1 + \xi^2} \tilde{\mathcal{R}}(d_c), \quad \xi = \frac{d}{d_c} \geq 1$$

Table of Contents

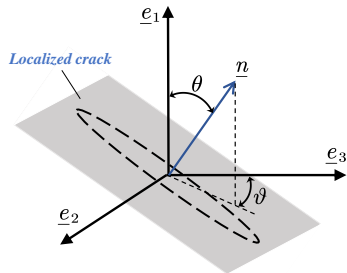
- 1 Motivation and objective
- 2 Micromechanics-based friction-damage model with pore pressure effect
- 3 Friction-damage modelling based on localized crack
- 4 Analysis of cracking localization**
- 5 Numerical simulation of porous quasi-brittle materials
- 6 Conclusions and perspectives

Onset of localized crack and orientation



Based on the critical damage, the corresponding microcrack-induced plastic strain at cracking localization:

$$\mathbf{E}^{c,l} = \int_0^{d_c} \lambda^c \mathbf{D} = \Lambda^{c,l} \mathbf{D} = d_c \sqrt{\frac{2\mathcal{R}(d_c)}{\chi}} \mathbf{D}$$



Critical plane:

$$\boldsymbol{\Sigma} = \Sigma_1 \mathbf{e}_1 \otimes \mathbf{e}_1 + \Sigma_2 \mathbf{e}_2 \otimes \mathbf{e}_2 + \Sigma_3 \mathbf{e}_3 \otimes \mathbf{e}_3$$

$$\mathbf{n}(\theta, \vartheta) = [\cos \theta, \sin \theta \sin \vartheta, \sin \theta \cos \vartheta]$$

The localized crack orientation verifies:

$$\tilde{\mathcal{F}}(\theta, \vartheta) = \|\underline{\tau}\| + \tilde{\eta}_f \Sigma_n + \tilde{\eta}_f P_w - \sqrt{\frac{2\tilde{\mathcal{R}}(d_c) \kappa^2}{\kappa_p}} = 0$$

$$\text{with } \kappa = \frac{c_t}{2} + \tilde{\eta}_f \tilde{\eta}_p c_n \text{ and } \kappa_p = \frac{c_t}{2} + \tilde{\eta}_p^2 c_n$$

Mohr's maximization postulate

The orientation of localized crack:

$$(\theta_c, \vartheta_c) = \arg \max \tilde{\mathcal{F}}(\theta, \vartheta)$$

The maximum condition:

$$\left. \frac{\partial \tilde{\mathcal{F}}(\theta, \vartheta)}{\partial (\theta, \vartheta)} \right|_{(\theta_c, \vartheta_c)} = \mathbf{0} ; \quad (\theta, \vartheta) \cdot \left. \frac{\partial^2 \tilde{\mathcal{F}}(\theta, \vartheta)}{\partial (\theta, \vartheta)^2} \right|_{(\theta_c, \vartheta_c)} \cdot (\theta, \vartheta) \leq 0, \quad \forall (\theta, \vartheta) \in \left[0, \frac{\pi}{2}\right]$$

Particular case of conventional triaxial conditions:

$$\mathbf{n}(\theta) = [\cos \theta, 0, \sin \theta]$$

- Macroscopic stresses

$$\Sigma_n = \underline{\mathbf{n}} \cdot \underline{\boldsymbol{\Sigma}} \cdot \underline{\mathbf{n}} = \Sigma_1 \cos^2 \theta + \Sigma_3 \sin^2 \theta$$

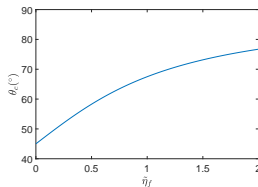
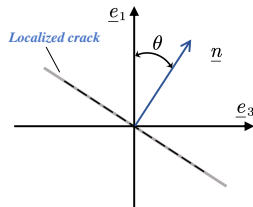
$$\|\underline{\boldsymbol{\tau}}\| = \|\underline{\boldsymbol{\Sigma}} \cdot \underline{\mathbf{n}} \cdot \mathbf{T}\| = (\Sigma_1 - \Sigma_3) \cos \theta \sin \theta$$

- Mohr's maximization postulate

$$\left. \frac{\partial \tilde{\mathcal{F}}(\theta)}{\partial \theta} \right|_{\theta_c} = 0 ; \quad \left. \frac{\partial^2 \tilde{\mathcal{F}}(\theta)}{\partial \theta^2} \right|_{\theta_c} \leq 0$$

with solution:

$$\theta_c = \arctan \left(\tilde{\eta}_f + \sqrt{1 + \tilde{\eta}_f^2} \right)$$



Analytical and semi-analytical solutions

At the initiation of localized crack:

$$\begin{cases} \mathcal{F}(\boldsymbol{\Sigma}, P_w, d_c) = \tilde{\mathcal{F}}(\boldsymbol{\Sigma}, P_w, d) \Big|_{d_c^+} \\ \boldsymbol{\Sigma}|_{d_c} = \boldsymbol{\Sigma}|_{d_c^+} \end{cases}$$

The analytical solution for drained tests while a semi-analytical solution for undrained conditions.

Drained conditions:

- ① Give a damage variable d at the beginning, compute the plastic multiplier Λ^c and the damage resistance $\mathcal{R}(d)$ (or $\tilde{\Lambda}^c$ and $\tilde{\mathcal{R}}(d)$, depending on $d > d_c$);
- ② Calculate the macroscopic axial stress Σ_1 by the confining stress Σ_3 and interstitial pressure P_w ;
- ③ Finally, obtain the macroscopic strain:

$$\mathbf{E} = \mathbb{S}^m : \boldsymbol{\Sigma} + \Lambda^c \mathbf{D} \quad \text{or} \quad \mathbf{E} = \mathbb{S}^m : \boldsymbol{\Sigma} + \Lambda^{cl} \mathbf{D} + \tilde{\Lambda}^c \mathbf{V}$$

Undrained conditions:

- ① Calculate the macroscopic stress-strain values by an trial value (at first $P_w^{\text{tr}} = P_{w,0}$);
- ② Then, substitute the plastic strain to obtain the current interstitial pressure $P_w^{\text{new}} = P_{w,0} + dP_w$;

- ③ Introducing a relative error:

$$\varpi^w = \left| \frac{P_w^{\text{tr}} - P_w^{\text{new}}}{P_w^{\text{tr}}} \right|$$

- ④ If $\varpi^w \leq \Pi^w$, accept results; otherwise, let $P_w^{\text{tr}} = P_w^{\text{new}}$ and return ① to recalculate.

Table of Contents

- 1 Motivation and objective
- 2 Micromechanics-based friction-damage model with pore pressure effect
- 3 Friction-damage modelling based on localized crack
- 4 Analysis of cracking localization
- 5 Numerical simulation of porous quasi-brittle materials**
- 6 Conclusions and perspectives

Drained triaxial tests for Sichuan sandstone

Table: Model parameters of Sichuan sandstone

E^m	ν^m	d_c	c_f	$\mathcal{R}(d_c)$	\tilde{c}_f	$\tilde{\mathcal{R}}(d_c)$	θ_c
20000MPa	0.2	1.8	1.01	0.069	0.59	0.086	60.42°

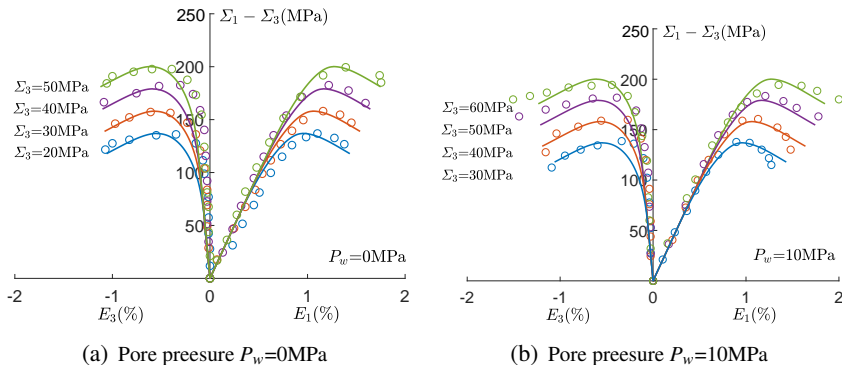
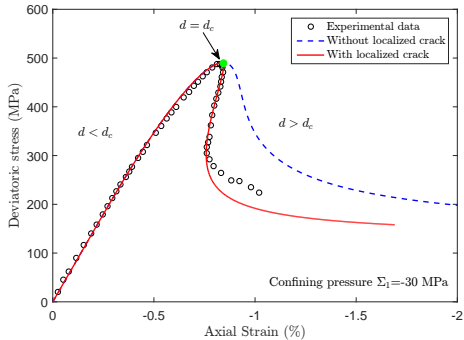
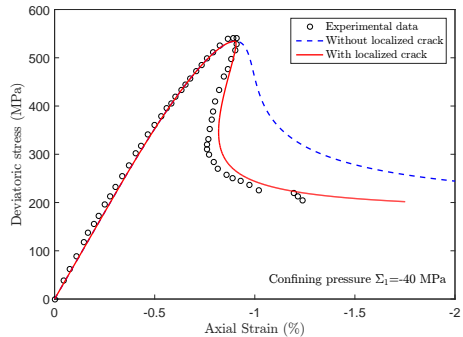


Figure: Experimental data and numerical results for triaxial drained compression tests on Sichuan sandstone

Application to Lac du Bonnet granite



(a) $P_c = 30$ MPa



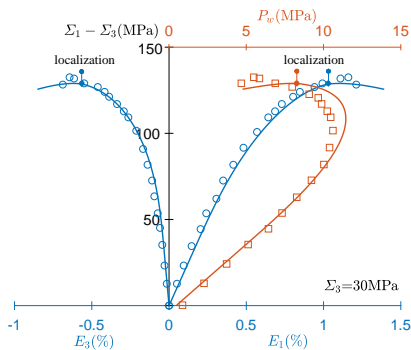
(b) $P_c = 40$ MPa

Figure: Analytical stress-strain curves of triaxial compression test on Lac du Bonnet granite with and without considering localized crack $\mathcal{R}(d) = \mathcal{R}_c \frac{b(d/d_c)}{b-1+(d/d_c)^b}$, $b > 1$

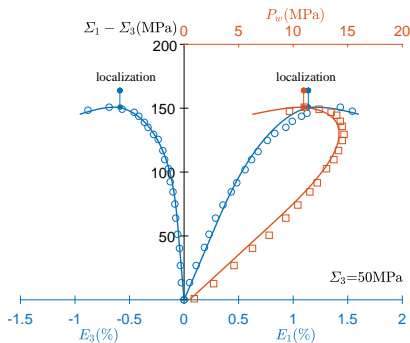
Undrained triaxial tests for Vosges sandstone

Table: Model parameters of Vosges sandstone

E^m	ν^m	d_c	c_f	$\mathcal{R}(d_c)$	\tilde{c}_f	$\tilde{\mathcal{R}}(d_c)$	θ_c	b	ϕ
20000MPa	0.2	1.5	0.73	0.13	0.42	0.14	56.40°	0.5	0.2



(a) Confining stress $\Sigma_3=30\text{MPa}$



(b) Confining stress $\Sigma_3=50\text{MPa}$

Figure: Experimental data and model numerical results for triaxial drained compression tests on Vosges stone

Triaxial tests for Hubei sandstone

Table: Model parameters of Hubei sandstone

Parameter	E^m	ν^m	d_c	c_f	$\mathcal{R}(d_c)$	\tilde{c}_f	$\tilde{\mathcal{R}}(d_c)$	θ_c	b	ϕ
Drained	18000MPa	0.23	1	1.001	0.046	0.59	0.057	60.30°	\	\
Undrained	21000MPa	0.23	1.3	0.61	0.16	0.35	0.18	54.70°	0.55	0.2

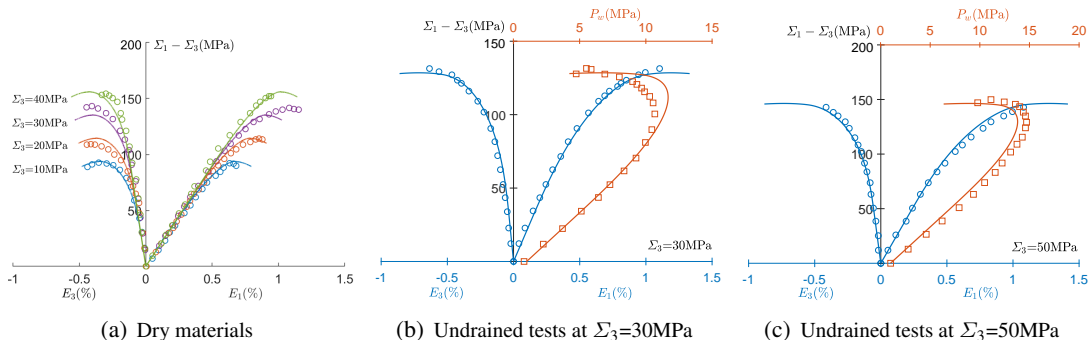
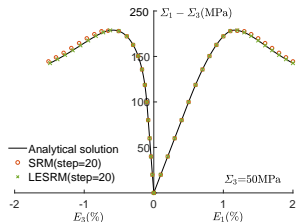
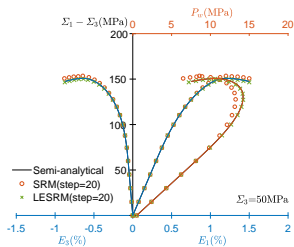


Figure: Experimental data and model numerical results for triaxial compression tests on Hubei stone

Local extended semi-implicit return mapping (LESRM) algorithm



(a) Drained tests of Sichuan sandstone



(b) Undrained tests of Vosges sandstone

Figure: Numerical algorithm results

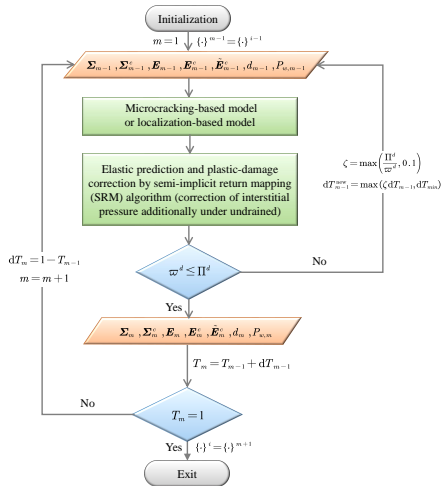


Figure: Flowchart of LESRM algorithm

Table of Contents

- 1 Motivation and objective
- 2 Micromechanics-based friction-damage model with pore pressure effect
- 3 Friction-damage modelling based on localized crack
- 4 Analysis of cracking localization
- 5 Numerical simulation of porous quasi-brittle materials
- 6 Conclusions and perspectives**

Conclusions and perspectives

Conclusions:

- Transition from diffuse micro-cracks to localized cracks.
- Pore pressure effect - effective stress concept.
- Coupling of friction-induced dilation - fluid pressure evolution.
- Verification for both drained and undrained tests.
- A novel algorithm for further numerical implementation.

Perspectives:

- Effective implementation for boundary values problems.
- Permeability change - cracking process.
- Extension to partially saturated media and THM problems.

Thanks for your attention